J. Fluid Mech. (1975), *vol.* 69, *part* 1, *pp.* 197–208
Printed in Great Britain

Source-sink flow in a gas centrifuge

By TAKUYA MATSUDA, TAKEO SAKURAI AND HIDENORI TAKEDA

Department of Aeronautical Engineering, Faculty of Engineering, Kyoto University, Kyoto, Japan

(Received 23 July 1974)

We consider steady non-axisymmetric source–sink flow of a perfect gas in a rapidly rotating circular cylinder for the case in which the sources and the sinks are distributed on the top and bottom. We apply a linearized analysis to a small perturbation from the state of rigid-body rotation. We show that the radial pressure gradient plays an important role in the determination of the axisymmetric part of the flow field and that the effects of viscosity and thermal conductivity govern the overall configuration of the non-axisymmetric part. We also show that the transport of gas in the main inner flow is axial and that radial transport is confined to the horizontal boundary layers.

1. Introduction

The study of gas flow in a rapidly rotating circular cylinder is important in relation to gas centrifuges used for the enrichment of uranium. Barcilon & Pedlosky (1967) and Homsy & Hudson (1969) studied this flow within the Boussinesq approximation. They delineated the parameter ranges in which the effect of thermal conduction is more important than that of thermal convection or vice versa, and gave a detailed discussion of the typical flow configurations. Sakurai & Matsuda (1974, henceforth referred to as I) showed that use of the Boussinesq approximation is not justified for practical cases, and proposed a widely applicable method of solution. Although these studies clarified many interesting aspects, they did not take into account the effect of the source–sink distribution, which is the crucial mechanical element of the gas centrifuge.

As was shown by Cohen (1951), we can calculate the separation power of a gas centrifuge of countercurrent type once we know the distribution of the axial velocity. Here, the distribution of the axial velocity is to be determined subject to the effect of the source–sink distribution on the cylinder walls. The effect of a side-wall distribution in the case of an incompressible fluid was studied by Barcilon (1967), Hide (1968) and Kuo & Veronis (1971), and we can find a review of their investigations in Greenspan (1968, p. 106). They showed that the transport of fluid from the source to the sink is restricted to the boundary layer in the case of a multiconnected region whereas this is not the case for a singly connected region.

Because some kinds of gas centrifuge have their source–sink distributions on the top and the bottom, it is necessary to study the effect of such distributions.

As is shown below, their effect has several aspects which are interesting from a purely gasdynamical viewpoint.

The problem studied in this paper is steady source–sink flow of a perfect gas in a circular cylinder which rotates around the vertical axis of symmetry and has source–sink distributions on the top and bottom. As in I, we assume that the angular velocity of the cylinder is so large that the radial pressure scale height is smaller than the radius of the cylinder whereas the vertical scale height is larger than the height of the cylinder. We assume that the viscosity and thermal conductivity are small and depend only on the temperature, and that the Prandtl number and the ratio of the radius to the height of the cylinder are of order unity.

In the formulation of the problem, we describe the source–sink distribution in terms of domains on which the axial component of the velocity is non-vanishing whereas the horizontal components do vanish. This property of the source–sink velocity is realized if the gas flows into or out of the cylinder through porous media. To avoid the appearance of vertical shear layers which affect the main inner flow, we assume that the magnitude of the non-dimensional source–sink velocity is of order $E^{\frac{1}{2}}$ (where E is the Ekman number) and the distributions of the axial velocity on the top and the bottom are sufficiently continuous functions of the plane variables r and θ. To avoid the appearance of a side-wall boundary layer, we also assume that the source–sink velocity vanishes on the periphery of the top and the bottom. We believe that subject to our restrictions the velocity field does not include any radical variations such as would occur across vertical shear layers; this is desirable from an engineering viewpoint. Finally, we assume that the temperature of the cylinder is uniform, because the effect of a temperature difference between the top and bottom is discussed in I and can be superposed on the present solution.

Before going directly into a discussion of the detailed mathematical treatment, we want to describe the main qualitative aspects of the non-dimensional flow. The flow field is decomposed into axisymmetric and non-axisymmetric parts.

First let us consider the axisymmetric part. Although the orders of magnitude of physical quantities are the same as those in I and the flow field is decomposed into a main inner flow and boundary layers similar to those in I, new aspects appear in relation to the source–sink distributions. Unlike the situation in I, an order-unity pressure gradient appears, corresponding to the driving of gas into or out of the cylinder. Through the thermo-geostrophic balance of forces, this pressure gradient causes an order-unity zonal motion in the main inner flow with respect to the cylinder. This zonal motion causes order-unity radial motion in the thermo-Ekman layers of thickness $E^{\frac{1}{2}}$ on the horizontal walls. As in I, the meridional motion in the main inner flow is axial, and causes order-$E^{\frac{1}{2}}$ mass transport between the top and bottom. As will be shown in § 3, the axial velocity of the main inner flow is the algebraic mean of the prescribed axial velocities on the top and bottom. This is exemplified for three typical cases in figures 1–3. For example, in figure 1, half of the mass injected at the source on the top penetrates into the main inner flow while the other half bifurcates into the top boundary layer. The former arrives at the bottom via the main inner flow and flows towards the suction point in the bottom boundary layer. The latter flows radially in the

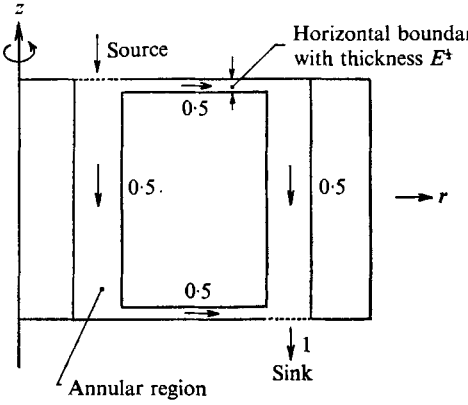

FIGURE 1. Meridional cross-section of the axisymmetric part of a source–sink flow. Arrows show the direction and numbers the magnitude of the mass flow.

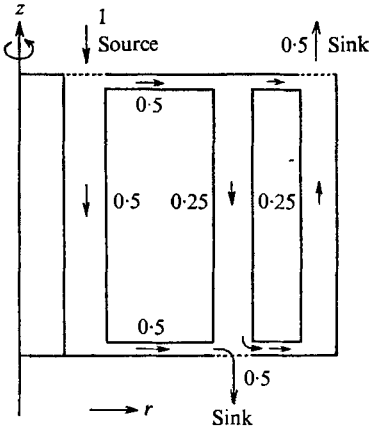

FIGURE 2. Meridional cross-section of the axisymmetric part of a source–sink flow of countercurrent type. Notation as in figure 1. The cut is assumed to be 0·5.

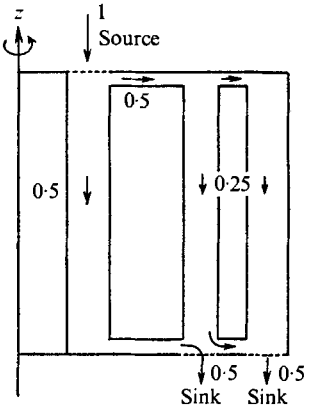

FIGURE 3. Meridional cross-section of the axisymmetric part of a source–sink flow of concurrent type. Notation as in figure 1. The cut is assumed to be 0·5.

top boundary layer up to the point just above the suction point on the bottom, and flows axially towards the suction point via the main inner flow. Other examples can be similarly interpreted. It is interesting that the above aspect of the mass transport is the same as that in incompressible flow. The zonal motion related to this axial motion, however, is different in the compressible case.

Let us next consider the non-axisymmetric part of the flow. Although this part can lead to no net mass transport, it is important in order to match the flow with the non-axisymmetric source–sink distributions. Because of the coupling with the axial component of the velocity, the zonal component is of order $E^{\frac{1}{2}}$, and there is no horizontal boundary layer which can carry the $E^{\frac{1}{2}}$ mass flux in the radial direction. Meridional motion is axial as in the axisymmetric part. An interesting point, however, is that the axial motion is not confined to annular regions enveloping the source–sink distributions. This is due to the fact that the effect of viscosity and thermal conductivity plays an important role in the determination of the flow field.

In §2, we give the basic equations and boundary conditions of the problem. We discuss the axisymmetric and non-axisymmetric parts of the flow in §§3 and 4, respectively.

2. Basic equations

Let us consider a system of cylindrical co-ordinates $(\tilde{r}, \theta, \tilde{z})$ fixed with respect to a circular cylinder rotating with angular velocity Ω around the vertical $(\tilde{z})$ axis, where tildes indicate physical (dimensional) quantities. If the temperature of the cylinder is uniform and equal to $\tilde{T}_0$ and there is no source–sink distribution, gas in the cylinder rotates rigidly with it. The pressure $\tilde{p}_R$ and density $\tilde{\rho}_R$ of this basic state of rigid-body rotation are as follows:

$$\tilde{p}_R = \tilde{p}_0 \epsilon_R, \quad \tilde{\rho}_R = \tilde{\rho}_0 \epsilon_R, \quad \tilde{p}_0 = \tilde{\rho}_0 R \tilde{T}_0, \tag{2.1}$$

$$\epsilon_R = \exp\left(\tilde{r}^2 \Omega^2 / 2R\tilde{T}_0 - g\tilde{z}/R\tilde{T}_0\right), \tag{2.2}$$

where R is the gas constant, g the acceleration due to gravity and the suffixes 0 and R refer to the point $\tilde{r} = \tilde{z} = 0$ and to the basic state of rigid-body rotation, respectively. As in I, the ratio of the cylinder radius to the radial pressure scale height $(= \tilde{r}^2\Omega^2/2R\tilde{T}_0)$ changes appreciably with $\tilde{r}$. For example, this ratio reaches 20 when UF_6 at 50 °C is placed in a rotating circular cylinder with a peripheral velocity of 400 m/s.

Using δ as a measure of the magnitude of the perturbation, L as the radius of the cylinder and H as the half-height of the cylinder, we introduce the following non-dimensional variables:

$$\left.\begin{aligned} (r, z) &= (\tilde{r}/L, \tilde{z}/H), \quad (u, v, w) = (\Omega L/\delta R T_0)\,(\tilde{q}_r, \tilde{q}_\theta, H\tilde{q}_z/L), \\ T &= (\tilde{T} - \tilde{T}_0)/\tilde{T}_0\delta, \quad p = (\tilde{p} - \tilde{p}_R)/\tilde{p}_R\delta, \quad \rho = (\tilde{\rho} - \tilde{\rho}_R)/\tilde{\rho}_R\delta, \end{aligned}\right\} \tag{2.3}$$

where $(\tilde{q}_r, \tilde{q}_\theta, \tilde{q}_z)$ is the dimensional velocity in cylindrical co-ordinates. It is to be noted that our present notation differs slightly from that in I. As a matter of course, however, the main procedures of the analysis are completely parallel.

By neglecting terms of higher order with respect to δ, we obtain linearized basic equations:

$$\frac{1}{r}\frac{\partial(ur)}{\partial r}+\frac{1}{r}\frac{\partial v}{\partial\theta}+\frac{\partial w}{\partial z}+G_0 ru-Gw=0, \tag{2.4}$$

$$-2v+G_0 rT+\frac{\partial p}{\partial r}=\frac{E}{\epsilon_R}\left(Lu+\frac{1}{3}\frac{\partial}{\partial r}\nabla\cdot\mathbf{V}-\frac{2}{r^2}\frac{\partial v}{\partial\theta}\right), \tag{2.5}$$

$$2u+\frac{1}{r}\frac{\partial p}{\partial\theta}=\frac{E}{\epsilon_R}\left(Lv+\frac{1}{3r}\frac{\partial}{\partial\theta}\nabla\cdot\mathbf{V}+\frac{2}{r^2}\frac{\partial u}{\partial\theta}\right), \tag{2.6}$$

$$-GT+\frac{\partial p}{\partial z}=\frac{E}{\epsilon_R}\left(\frac{1}{A^2}\Delta w+\frac{1}{3}\frac{\partial}{\partial z}\nabla\cdot\mathbf{V}\right), \tag{2.7}$$

$$\frac{\gamma-1}{\gamma}P_r\left(-ru+\frac{G}{G_0}w\right)=\frac{E}{\epsilon_R}\Delta T, \tag{2.8}$$

$$p=\rho+T, \tag{2.9}$$

where

$$\left.\begin{aligned}&\Delta=\frac{\partial^2}{\partial r^2}+\frac{1}{r}\frac{\partial}{\partial r}+\frac{1}{r^2}\frac{\partial^2}{\partial\theta^2}+A^2\frac{\partial^2}{\partial z^2},\quad L=\Delta-\frac{1}{r^2},\\&E=\frac{\tilde{\mu}_0}{\tilde{\rho}_0\Omega L^2},\quad G_0=\frac{\Omega^2L^2}{R\tilde{T}_0},\quad G=\frac{gH}{R\tilde{T}_0},\quad A=\frac{L}{H}\end{aligned}\right\} \tag{2.10}$$

and P_r is the Prandtl number, γ the ratio of the specific heats, μ the viscosity, E the Ekman number, G_0 the ratio of the cylinder radius to the radial scale height on the side wall, G the ratio of the cylinder half-height to the vertical scale height, and A the aspect ratio, i.e. the ratio of the radius to the half-height of the cylinder. The above equations differ from those in I in that they include derivatives with respect to θ. If we assume that $L=10\,\text{cm}$, $H=50\,\text{cm}$, $\Omega L=400\,\text{m/s}$, $\tilde{T}_0=50\,^\circ\text{C}$ and $p=100\,\text{mm Hg}$ on the side wall, we obtain $E\sim10^{-2}$, $G\sim10^{-3}$, $G_0\sim20$ and $A\sim0{\cdot}2$. For the sake of simplicity, we restrict ourselves to the case $G\ll E^{\frac{1}{2}}$ as in I and neglect the effect of the gravity.

The boundary conditions are

$$u=v=T=0\begin{cases}\text{on}\quad r=1,\quad -1\leqslant z\leqslant 1,\\ \text{on}\quad z=\pm1,\quad 0\leqslant r\leqslant 1,\end{cases} \tag{2.11}$$

$$w=\left.\begin{cases}w_T(r,\theta)&\text{on}\quad z=1,\quad 0\leqslant r\leqslant 1,\\ w_B(r,\theta)&\text{on}\quad z=-1,\quad 0\leqslant r\leqslant 1,\\ 0&\text{on}\quad r=1,\quad -1\leqslant z\leqslant 1.\end{cases}\right\} \tag{2.12}$$

The source–sink distributions w_T and w_B can be decomposed as

$$w_{T(B)}(r,\theta)=w_{T(B)S}(r)+w_{T(B)N}(r,\theta), \tag{2.13}$$

where

$$w_{T(B)S}(r)=\frac{1}{2\pi}\int_0^{2\pi}w_{T(B)}(r,\theta)\,d\theta \tag{2.14}$$

and suffixes S and N refer to the axisymmetric and non-axisymmetric parts, respectively. The flow is also decomposed correspondingly. We shall discuss the axisymmetric part in §3 and the non-axisymmetric part in §4.

3. Axisymmetric part

The basic equations and the decomposition of the flow field into a main inner flow and boundary-layer flow are the same as those in I except that a side-wall boundary layer does not appear by our simplifying assumption.

Main inner flow

Because w is of order $E^{\frac{1}{2}}$, the scaling is as follows:

$$\left.\begin{aligned} u_i = E^{-1}u, \quad v_i = v, \quad w_i = E^{-\frac{1}{2}}w, \\ T_i = T, \quad p_i = p, \quad \rho_i = \rho, \end{aligned}\right\} \tag{3.1}$$

where the suffix i refers to the main inner flow, quantities with this suffix being of order unity. Substitution of (3.1) into the axisymmetric part of (2.4)–(2.9) yields

$$\partial w_i/\partial z = 0, \tag{3.2}$$

$$v_i = \frac{G_0 r T_i}{2} + \frac{1}{2}\frac{\partial p_i}{\partial r}, \quad u_i = \frac{1}{2\epsilon_R} L v_i, \tag{3.3), (3.4}$$

$$\partial p_i/\partial z = 0, \tag{3.5}$$

$$-ru_i = (G_0/4h\epsilon_R)\,\Delta T_i, \tag{3.6}$$

$$p_i = \rho_i + T_i, \tag{3.7}$$

where

$$h = (\gamma - 1)\,P_r G_0/4\gamma. \tag{3.8}$$

Standard elimination among (3.3)–(3.6) gives

$$(1+hr^2)\left(\frac{\partial^2}{\partial r^2} + A^2\frac{\partial^2}{\partial z^2}\right)T_i + \frac{1+3hr^2}{r}\frac{\partial T_i}{\partial r} = \frac{hr}{G_0} L f(r), \tag{3.9}$$

where

$$f(r) = -\partial p/\partial r. \tag{3.10}$$

Equation (3.9) is the same as equation (3.9) of I, except for the right-hand side and the factor A^2 multiplying $\partial^2 T_i/\partial z^2$. The right-hand side corresponds to the driving of gas into and out of the cylinder and is crucial in the problem of source–sink flow. This term itself is to be determined by the boundary conditions on the cylinder wall.

Horizontal boundary layers

The scaling for the boundary-layer flow is as follows:

$$\left.\begin{aligned} \hat{u} = u, \quad \hat{v} = v, \quad \hat{w} = E^{-\frac{1}{2}}w, \quad \hat{T} = T, \quad \hat{\rho} = \rho, \quad \hat{p} = E^{-1}p, \\ \eta = E^{-\frac{1}{2}}j(j-z) \quad (j = \pm 1), \end{aligned}\right\} \tag{3.11}$$

where carets refer to the horizontal boundary layers, and $j = \pm 1$ to the top and bottom, respectively, the quantities with carets being of order unity. Substitution of (3.11) into the axisymmetric version of (2.4)–(2.9) gives

$$\frac{1}{r}\frac{\partial(r\hat{u})}{\partial r} - j\frac{\partial \hat{w}}{\partial \eta} + G_0 r\hat{u} = 0, \tag{3.12}$$

$$2\hat{v} = G_0 r\hat{T} - \frac{A^2}{\epsilon_R}\frac{\partial^2 \hat{u}}{\partial \eta^2}, \quad 2\hat{u} = \frac{A^2}{\epsilon_R}\frac{\partial^2 \hat{v}}{\partial \eta^2}, \tag{3.13), (3.14}$$

$$-j\frac{\partial\hat{p}}{\partial\eta}=\frac{1}{\epsilon_R}\left\{\frac{4}{3}\frac{\partial^2\hat{w}}{\partial\eta^2}-\frac{j}{3r}\frac{\partial}{\partial r}\left(r\frac{\partial\hat{u}}{\partial\eta}\right)\right\}, \tag{3.15}$$

$$r\hat{u}=-\frac{A^2G_0}{4h\epsilon_R}\frac{\partial^2\hat{T}}{\partial\eta^2}, \tag{3.16}$$

$$\hat{p}+\hat{T}=0. \tag{3.17}$$

The boundary conditions on the horizontal walls are

$$\hat{u}=\hat{v}+v_i=\hat{T}+T_i=0 \quad \text{on} \quad z=\pm 1, \quad 0\leqslant r\leqslant 1, \tag{3.18a–c}$$

$$\hat{w}+w_i=\begin{cases}w_{TS}(r) & \text{on} \quad z=+1, \quad 0\leqslant r\leqslant 1,\\ w_{BS}(r) & \text{on} \quad z=-1, \quad 0\leqslant r\leqslant 1.\end{cases} \tag{3.19}$$

Elimination of $\hat{u}$ from (3.14) and (3.16), subject to the boundary conditions as $\eta\to\infty$, gives

$$\hat{v}=-G_0\hat{T}/2hr. \tag{3.20}$$

Substitution of (3.3) and (3.20) into (3.18) yields

$$T_i(z=\pm 1)=\frac{hr}{G_0(1+hr^2)}f(r), \quad \hat{T}(\eta=0)=-\frac{hr}{G_0(1+hr^2)}f(r), \tag{3.21}$$

which show that the boundary conditions on the main inner flow and the boundary-layer flow can be determined from the radial pressure gradient.

Elimination of $\hat{v}$ and $\hat{T}$ from (3.13), (3.14) and (3.20) gives

$$\partial^4\hat{u}/\partial\eta^4+4\sigma^4\hat{u}=0, \tag{3.22}$$

where

$$\sigma=\{\epsilon_R^2(1+hr^2)\}^{\frac{1}{4}}/A. \tag{3.23}$$

The solution of this equation subject to (3.18*a*) and (3.21) is as follows:

$$\hat{u}=\frac{f(r)}{2(1+hr^2)^{\frac{1}{2}}}e^{-\sigma\eta}\sin\sigma\eta, \tag{3.24}$$

$$\hat{T}=-\frac{hrf(r)}{G_0(1+hr^2)}e^{-\sigma\eta}\cos\sigma\eta. \tag{3.25}$$

In contrast to the solution in I, $\hat{u}$ and $\hat{T}$ are symmetric with respect to $z=0$. Thus, by (3.12), $\hat{w}$ is antisymmetric with respect to $z=0$. This reflects the fact that the present source–sink flow is driven by the radial pressure gradient related to the source and the sink whereas the flow in I is driven by the antisymmetric temperature gradient. Because of this symmetry character, (3.19) gives

$$w_i=\tfrac{1}{2}(w_{TS}+w_{BS}), \tag{3.26}$$

$$\hat{w}(\eta=0)=\tfrac{1}{2}j(w_{TS}-w_{BS}). \tag{3.27}$$

The function $\hat{w}$ is obtained by integration of (3.12) as

$$\hat{w}=\frac{j}{4\sigma(1+hr^2)^{\frac{1}{2}}}\left\{f'+f\left(\frac{1}{r}+\frac{G_0r}{2}-\frac{3}{2}\frac{hr}{1+hr^2}\right)\right\}e^{-\sigma\eta}(\cos\sigma\eta+\sin\sigma\eta)$$
$$-\frac{jf}{4(1+hr^2)^{\frac{1}{2}}}\left(G_0r+\frac{hr}{1+hr^2}\right)\eta\,e^{-\sigma\eta}\sin\sigma\eta. \tag{3.28}$$

Substitution of (3.28) into (3.27) gives

$$f' + \left(\frac{1}{r} + \frac{G_0 r}{2} - \frac{3}{2}\frac{hr}{1+hr^2}\right) f = 2\sigma(1+hr^2)^{\frac{1}{2}}(w_{TS} - w_{BS}). \tag{3.29}$$

Because f does not have a singularity at $r = 0$, the integration of (3.29) is straightforward:

$$f = \frac{2}{A}\frac{(1+hr^2)^{\frac{3}{4}}}{r}\exp(-\tfrac{1}{4}G_0 r^2)\int_0^r s(w_{TS} - w_{BS})\exp(\tfrac{1}{2}G_0 s^2)\,ds. \tag{3.30}$$

From (3.30) we can obtain f, and thus the boundary values of T_i, once the source–sink distributions w_{TS} and w_{BS} on the top and the bottom have been prescribed. As for the boundary condition on the side wall, let us first verify that $f(r)$ vanishes at $r = 1$ by the requirement of mass conservation. Provided that T_i vanishes on the side wall, so does v_i. If the source–sink velocity vanishes at $r = 1$, so does w_i by (3.26). Because u_i is of higher order with respect to E, the non-vanishing u_i can be adjusted by the higher-order side-wall boundary layer. Therefore, the side-wall boundary condition at lowest order is

$$T_i = 0 \quad \text{on} \quad r = 1, \quad -1 \leqslant z \leqslant 1. \tag{3.31}$$

The solution for the main inner flow

Substitution of

$$T_i = T_0(r) + \sum_{n=1}^{\infty} \frac{\cosh \lambda_n z}{\cosh \lambda_n} T_n(r) \tag{3.32}$$

into (3.9) and (3.31) gives

$$(1+hr^2)T_0'' + \frac{1+3hr^2}{r}T_0' = hF(r), \tag{3.33}$$

$$(1+hr^2)T_n'' + \frac{1+3hr^2}{r}T_n' + A^2\lambda_n^2 T_n = 0, \tag{3.34}$$

$$F(r) = \frac{r}{G_0}Lf = \frac{r}{G_0}\left(f'' + \frac{1}{r}f' - \frac{f}{r^2}\right), \tag{3.35}$$

$$T_0 = T_n = 0 \quad \text{on} \quad r = 1, \tag{3.36}$$

where primes denote differentiation with respect to r and λ_n is an eigenvalue to be determined by (3.36).

Because T_0 is finite at $r = 0$, the solution of (3.33) subject to (3.36) is

$$T_0(r) = -h\int_r^1 \frac{dt}{t(1+ht^2)}\int_0^t sF(s)\,ds \tag{3.37a}$$

$$= hT_{00} + h^2 T_{01} + O(h^3), \tag{3.37b}$$

with

$$T_{00} = \frac{1}{G_0}\left\{rf + 2\int_r^1 f(t)\,dt\right\}, \tag{3.38}$$

$$T_{01} = -\frac{1}{G_0}\left\{r^3 f + 4\int_r^1 t^2 f(t)\,dt\right\}, \tag{3.39}$$

where (3.37*b*) is an expansion, as in I, with respect to h.

Similar expansions of T_n and λ_n with respect to h,

$$T_n(r) = hT_{n0} + h^2 T_{n1} + O(h^3), \tag{3.40}$$

$$\lambda_n = \lambda_{n0} + h\lambda_{n1} + O(h^2), \tag{3.41}$$

give

$$T''_{n0} + r^{-1}T'_{n0} + A^2\lambda_{n0}^2 T_{n0} = 0, \tag{3.42}$$

$$T''_{n1} + r^{-1}T'_{n1} + A^2\lambda_{n0}^2 T_{n1} = -2A^2\lambda_{n1}\lambda_{n0}T_{n0} - 2rT'_{n0}, \tag{3.43}$$

$$T_{n0} = T_{n1} = 0 \quad \text{at} \quad r = 1. \tag{3.44}$$

Because (3.42)–(3.44) are the same as equations (4.6)–(4.8) of I, the solutions can be expressed as

$$T_{n0} = a_{n0}J_0(A\lambda_{n0}r), \quad T_{n1} = (a_{n1} - \tfrac{1}{2}r^2 a_{n0})\,J_0(A\lambda_{n0}r), \tag{3.45}$$

$$\lambda_{n0} = j_{0n}/A, \quad \lambda_{n1} = 1/\lambda_{n0}, \tag{3.46}$$

where J_0 is the zeroth-order Bessel function, j_{0n} the nth zero of J_0, and the constants a_{n0} and a_{n1} are to be determined from the boundary conditions (3.21) on the top and bottom. The boundary conditions (3.21) are expanded with respect to h as

$$T_i = hrf/G_0 - h^2 r^3 f/G_0 + O(h^3) \quad \text{on} \quad z = \pm 1, \quad 0 \leqslant r \leqslant 1. \tag{3.47}$$

Substitution of (3.37)–(3.39), (3.32) and (3.40) into (3.47) gives

$$\sum_{n=1}^{\infty} a_{n0}J_0(j_{0n}r) = -\frac{2}{G_0}\int_r^1 f(t)\,dt,$$

$$\sum_{n=1}^{\infty}\left(a_{n1} - \frac{r^2}{2}a_{n0}\right)J_0(j_{0n}r) = \frac{4}{G_0}\int_r^1 t^2 f(t)\,dt. \tag{3.48}$$

Because $\{J_0(j_{0n}r)\}$ is an orthogonal set of functions in $0 \leqslant r \leqslant 1$, the coefficients a_{n0} and a_{n1} can be calculated by standard methods.

Substitution of the above results into (3.32) yields, after a little manipulation,

$$\begin{aligned} T_i = {} & h\left\{T_{00} + \sum_{n=1}^{\infty}\frac{\cosh\lambda_{n0}z}{\cosh\lambda_{n0}}a_{n0}J_0(j_{0n}r)\right\} \\ & + h^2\left[T_{01} + \sum_{n=1}^{\infty}\frac{\cosh\lambda_{n0}z}{\cosh\lambda_{n0}}\{a_{n1} - \tfrac{1}{2}r^2 a_{n0} + \lambda_{n1}a_{n0}(z\tanh\lambda_{n0}z - \tanh\lambda_{n0})\}\right. \\ & \left.\times J_0(j_{0n}r)\right] + O(h^3). \end{aligned} \tag{3.49}$$

4. Non-axisymmetric part

Substitution of the scaling

$$\left.\begin{aligned} u &= E^{\frac{3}{2}}\sum_m{}' u_m e^{im\theta}, \quad v = E^{\frac{1}{2}}\sum_m{}' v_m e^{im\theta}, \quad w = E^{\frac{1}{2}}\sum_m{}' w_m e^{im\theta}, \\ T &= E^{\frac{1}{2}}\sum_m{}' T_m e^{im\theta}, \quad \rho = E^{\frac{1}{2}}\sum_m{}' \rho_m e^{im\theta}, \quad p = E^{\frac{3}{2}}\sum_m{}' p_m e^{im\theta} \end{aligned}\right\} \tag{4.1}$$

into (2.4)–(2.9) gives

$$v_m = \frac{ir}{m}\frac{\partial w_m}{\partial z} = \frac{G_0 r}{2} T_m, \tag{4.2), (4.3}$$

$$2u_m + \frac{im}{r} p_m = \frac{1}{\epsilon_R} L v_m, \tag{4.4}$$

$$\frac{\partial p_m}{\partial z} = \frac{1}{A^2 \epsilon_R} \Delta w_m, \tag{4.5}$$

$$u_m = -\frac{\gamma}{(\gamma - 1) P_r r \epsilon_R} \Delta T_m, \tag{4.6}$$

$$0 = \rho_m + T_m, \tag{4.7}$$

where primes indicate summation with respect to non-zero m, the suffix m refers to the mth complex Fourier coefficient, and quantities with a suffix m are of order unity. In these equations, terms of lowest order with respect to E are retained, G is omitted for the sake of simplicity and Δ is the version of the Laplacian corresponding to the mth complex Fourier coefficient.

Because the zonal velocity is of order $E^{\frac{1}{2}}$, there can exist no horizontal boundary layers which, for example, adjust the non-vanishing axial velocity component such that it vanishes on the boundary. This situation can be remedied as the effect of viscosity is retained in the zonal and axial components of the momentum equations and the thermal conductivity is retained in the energy equation [see (4.4)–(4.6)]. The boundary conditions (2.11) and (2.12) can be combined with the above system of equations to compose a well-posed problem. Elimination among the above equations gives

$$\Delta \frac{\partial^2 w_m}{\partial z^2} = h \left\{ \frac{m^2}{A^2} \Delta w_m - rLr \frac{\partial^2 w_m}{\partial z^2} \right\}. \tag{4.8}$$

Because the differentiation with respect to z is of fourth order, we can prescribe two boundary values on the top and the bottom. These are

$$\left.\begin{aligned} w_m &= \begin{cases} w_{Tm} & \text{on} \quad z = 1, \\ w_{Bm} & \text{on} \quad z = -1, \end{cases} \\ \partial w_m / \partial z &= 0 \quad \text{on} \quad z = \pm 1, \quad 0 \leqslant r \leqslant 1. \end{aligned}\right\} \tag{4.9}$$

Because u_m is of higher order with respect to E, the boundary conditions on u_m can be adjusted by higher-order horizontal boundary layers. Next, if w_m vanishes on horizontal walls, so do v_m and T_m by (4.2) and (4.3). Therefore, the lowest-order boundary conditions on the side wall are

$$w_m = 0 \quad \text{on} \quad r = 1, \quad -1 \leqslant z \leqslant 1. \tag{4.10}$$

Substitution of the expansion with respect to h,

$$w_m = w_{m0} + h w_{m1} + \ldots, \tag{4.11}$$

into (4.8) gives us the lowest-order equation:

$$\Delta \, \partial^2 w_{m0} / \partial z^2 = 0. \tag{4.12}$$

The solution of this equation can be written as

$$w_{m0} = g_1(r) + zg_2(r) + \sum_{n=1}^{\infty} J_m(A\lambda_{mn}r)\{a_{m0n}\sinh[\lambda_{mn}(z+1)] + b_{m0n}\sinh[\lambda_{mn}(z-1)]\}, \quad (4.13)$$

where J_m is the mth-order Bessel function and λ_{mn}, a_{m0n} and b_{m0n} are coefficients to be determined by the boundary conditions. Substitution of (4.13) into (4.10) gives

$$g_1(1) = g_2(1) = J_m(A\lambda_{mn}) = 0. \quad (4.14)$$

From this boundary condition,

$$\lambda_{mn} = j_{m,n}/A, \quad (4.15)$$

where $j_{m,n}$ is the nth zero of J_m. Before discussing the boundary conditions on the horizontal walls, let us note that $\{J_m(j_{m,n}r)\}$ is an orthogonal set of functions in $0 \leqslant r \leqslant 1$, and the source–sink distribution can be expanded in this set:

$$w_{Tm} = \sum_{n=1}^{\infty} A_{Tmn}J_m(j_{m,n}r) \quad \text{on} \quad z = +1, \quad (4.16)$$

$$w_{Bm} = \sum_{n=1}^{\infty} A_{Bmn}J_m(j_{m,n}r) \quad \text{on} \quad z = -1. \quad (4.17)$$

Substitution of (4.13) into (4.9) gives

$$\left.\begin{aligned} g_1 &= \tfrac{1}{2}(w_{Tm} + w_{Bm}), \\ g_2 &= -\sum_{n=1}^{\infty} \frac{j_{m,n}}{A} a_{m0n}J_m(j_{m,n}r)(\cosh 2\lambda_{mn} + 1), \\ a_{m0n} &= b_{m0n} = \frac{A_{Bmn} - A_{Tmn}}{2\{\lambda_{mn}[\cosh(2\lambda_{mn}) + 1] - \sinh 2\lambda_{mn}\}}. \end{aligned}\right\} \quad (4.18)$$

The higher-order terms with respect to h can be obtained by the same procedure.

This paper is dedicated to Professor Isao Imai in celebration of his sixtieth birthday. The authors wish to express their thanks to Mr K. Hashimoto for his critical discussion of their results.

Note. After the completion of this manuscript, a paper by Nakayama & Usui (1974) reporting similar theoretical work on source–sink flow in a gas centrifuge appeared. They treated the case of point injection, and their mathematical treatment is concentrated on the flow in the vertical shear layer. Our present study, in contrast, treats the case of injection over a finite area, and our mathematical treatment is concentrated on the main inner flow subject to the effect of a non-axisymmetric distribution of sources and sinks.

REFERENCES

BARCILON, V. 1967 On the motion due to sources and sinks distributed along the vertical boundary of a rotating fluid. *J. Fluid Mech.* **27**, 551–560.

BARCILON, V. & PEDLOSKY, J. 1967 On the steady motions produced by a stable stratification in a rapidly rotating fluid. *J. Fluid Mech.* **29**, 673–690.

COHEN, K. 1951 *The Theory of Isotope Separation as Applied to the Large-Scale Production of* U^{235}. McGraw-Hill.

GREENSPAN, H. P. 1968 *The Theory of Rotating Fluids*. Cambridge University Press.

HIDE, R. 1968 On source–sink flows in a rotating fluid. *J. Fluid Mech.* **32**, 737–764.

HOMSY, G. M. & HUDSON, J. L. 1969 Centrifugally driven thermal convection in a rotating cylinder. *J. Fluid Mech.* **35**, 33–52.

KUO, H.-H. & VERONIS, G. 1971 The source–sink flow in a rotating system and its oceanic analogy. *J. Fluid Mech.* **45**, 441–464.

NAKAYAMA, W. & USUI, S. 1974 Flow in rotating cylinder of a gas centrifuge. *J. Nucl. Sci. Tech.* **11**, 242–262.

SAKURAI, T. & MATSUDA, T. 1974 Gasdynamics of a centrifugal machine. *J. Fluid Mech.* **62**, 727–736.